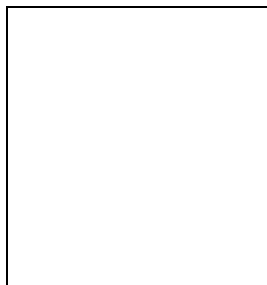


## PHOTON STRUCTURE AT HERA

H. JUNG

*Department of Physics, Lund University, 221 00 Lund, Sweden*

*For the H1 and ZEUS Collaborations*



The structure of the virtual photon and its contribution to small  $x$  processes in deep inelastic scattering at HERA is discussed.

### 1 Introduction

In electron-proton scattering the internal structure of the proton as well as of the exchanged photon can be resolved provided the scale  $\mu^2$  of the hard subprocess is larger than the inverse size of the proton,  $1/R_p^2 \sim \Lambda_{QCD}^2$ , and inverse size of the photon,  $1/R_\gamma^2 \sim Q^2$ , respectively. Resolved photon processes play an important role in photo-production of high  $E_T$  jets<sup>1,2</sup>, where  $Q^2 \approx 0$ , but they can also give considerable contributions to DIS processes<sup>3,4</sup>. if the scale  $\mu^2$  of the hard subprocess is larger than  $Q^2$ . In the following I shall discuss the role of resolved virtual photons in small  $x$   $ep$  scattering.

### 2 Small $x$ parton dynamics and the structure of the virtual photon

The cross section at low  $x$  and large  $Q^2$  with a high  $p_T^2$  jet in the proton direction (a forward jet) has been advocated as a particularly sensitive measure of small  $x$  parton dynamics<sup>5,6</sup>. If the forward jet has large energy ( $x_{jet} = E_{jet}/E_{proton} \gg x$ ) the evolution from  $x_{jet}$  to small  $x$  can be studied. When  $E_T^2 \sim Q^2$  there is no room for  $Q^2$  evolution left and the DGLAP formalism predicts a rather small cross section in contrast to the BFKL formalism, which describes the evolution in  $x$ . More information about the underlying parton dynamics can be obtained by a measurement of the forward jet cross section as a function of the ratio  $E_T^2/Q^2$ . Three interesting regions of phase space can be defined:

- $E_T^2 < Q^2$  “standard” DIS region (direct photon processes),  $Q^2$  is the largest scale in the process

- $E_T^2 \simeq Q^2$  BFKL region, two scale problem.
- $E_T^2 > Q^2$  “resolved  $\gamma^*$ ” region,  $E_T^2$  is the largest scale, similar to photo-production processes.

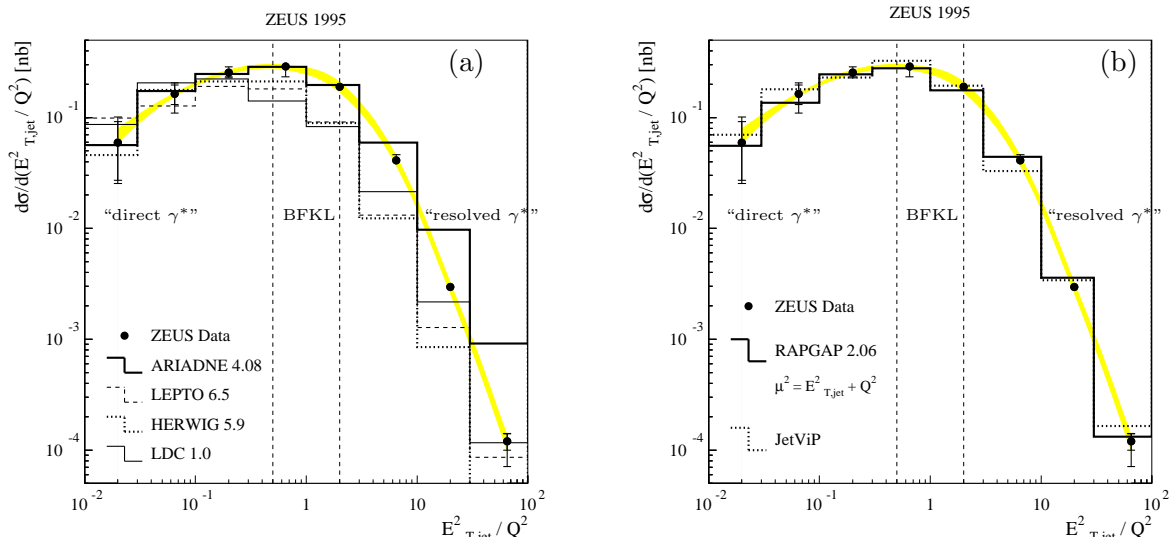


Figure 1: The forward jet cross section as a function of  $E_T^2/Q^2$  in the region  $Q^2 > 10 \text{ GeV}^2$ ,  $\eta_{jet} < 2.6$ ,  $E_{t jet} > 5 \text{ GeV}$ ,  $x_{jet} > 0.036$ . The shaded band shows the hadronic energy scale uncertainty. In *a* predictions from standard deep inelastic Monte Carlo generators are shown. In *b* the prediction from a Monte Carlo generator and a full NLO calculation including resolved virtual photons are shown<sup>7</sup>. Indicated are also the three different regions of phase space defined in the text.

The forward jet cross section as a function of  $E_T^2/Q^2$ <sup>8</sup> is shown in Fig.1. In Fig 1a the data are compared with predictions from standard deep inelastic Monte Carlo programs, LEPTO<sup>9</sup> and HERWIG<sup>10</sup> which use direct photon processes only. The cross section in the standard deep inelastic region  $E_T^2 < Q^2$  is reasonably well described, but in the other regions underestimated by large factors. In Fig 1b the data are compared with predictions including also processes from resolved virtual photons. The data are well described over the full phase space. It should be noted that only the anomalous component of the resolved virtual photon contributes significantly at large  $Q^2$  (which can be calculated in pQCD), whereas the vector meson component becomes negligible. Thus a reasonable approximation to small  $x$  parton dynamics can be achieved by adding a resolved virtual photon contribution to the direct photon processes. By doing this, a situation similar to BFKL is obtained: The transverse momenta of the emitted partons need no longer be ordered in transverse momentum, since in a resolved photon process there are two DGLAP ladders, one from the photon and one from the proton towards the hard scattering matrix element. However in order to achieve such a good description of the data, the scale  $\mu^2$  for the hard subprocess has to be sufficiently large, e.g.  $\mu^2 = Q^2 + p_T^2$  or  $\mu^2 = 4p_T^2$ , as was shown in<sup>11</sup>. If the scale is chosen to be  $\mu^2 = p_T^2$ , the predictions fall below the data. In that case there is only a small contribution from resolved virtual photons. Thus to successfully also describe the BFKL region, a (artificial) sufficiently large scale  $\mu^2$  has to be chosen to simulate enough high  $p_T$  emissions.

### 3 Structure of virtual photons

In photo-production the high  $E_T$  di-jet cross section has been extensively used to study the structure of the real photon as a function of  $x_\gamma$ , in LO the fraction of the photon momentum

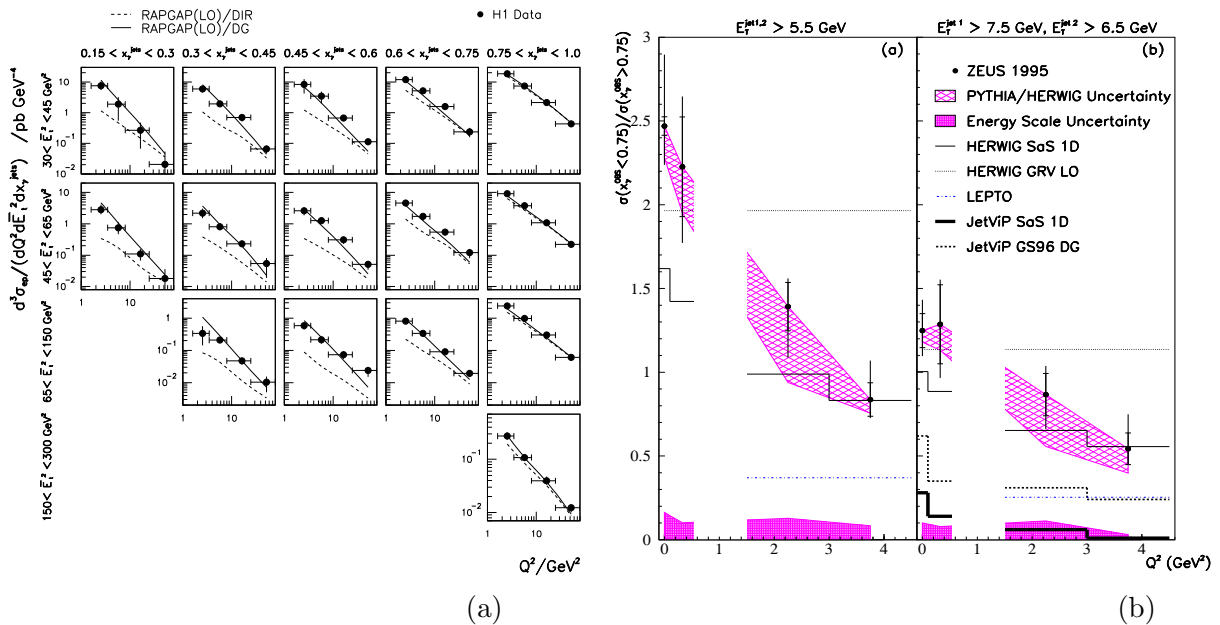


Figure 2: *a*. The cross section of di-jet production<sup>12</sup> as a function of  $Q^2$  in bins of  $x_\gamma$  and  $E_T^2$  in the kinematic range of  $0.1 < y < 0.7$  and di-jets found with the inclusive  $k_T$  jet algorithm with  $\bar{E}_T^2 > 30 \text{ GeV}^2$ . Also shown is the Monte Carlo prediction for the direct photon contribution alone (dashed line) and the sum of direct and resolve photon processes (solid line). *b*. The ratio  $R = \sigma^{\text{resolved}}/\sigma^{\text{direct}}$ <sup>13</sup> as a function of  $Q^2$  for the low and high  $E_T$  sample. Also shown are the predictions from the HERWIG Monte Carlo program including a contribution of resolved photons and a NLO calculation<sup>14</sup>.

carried by the parton<sup>1,2</sup>. High  $E_T$  di-jet production at  $Q^2 > 0$  can be used to determine the structure of the virtual photon, if  $E_T^2 > Q^2$ . Such studies have been performed by H1<sup>12</sup> and ZEUS<sup>13</sup>. In Fig. 2a the di-jet cross section is shown as a function of  $Q^2$  for different bins in  $x_\gamma$  and  $E_T$  together with a Monte Carlo prediction of direct photon processes and the sum of direct and resolved virtual photons. In the region of small  $x_\gamma$  and small  $Q^2$  the measured cross section lies far above the prediction involving direct virtual photons only. This indicates that additional processes are needed to explain the data. Including in addition contributions from resolved virtual photon processes a reasonable description of the data is obtained. The contribution of resolved virtual photons is largest for  $Q^2 \ll E_T^2$  and  $x_\gamma \ll 1$ . A complementary measurement has been performed by ZEUS<sup>13</sup> measuring di-jet cross section in the region  $0 < Q^2 < 4.5 \text{ GeV}^2$  for two different regions in  $x_\gamma$ , the direct photon region ( $x_\gamma > 0.75$ ) and the resolved photon region ( $x_\gamma < 0.75$ ). In Fig. 2b the ratio  $R = \sigma^{\text{resolved}}/\sigma^{\text{direct}}$  as a function of  $Q^2$  is shown for a low  $E_T$  ( $E_T > 5.5 \text{ GeV}$ ) and a high  $E_T$  ( $E_{T1} > 7.5 \text{ GeV}$  and  $E_{T2} > 6.5 \text{ GeV}$ ) sample. The high  $E_T$  sample is much less influenced by multiple interactions compared to the low  $E_T$  sample. Also here a significant contribution over the standard direct photon processes are needed to describe the data. Thus we can conclude that in the region of  $E_T^2 > Q^2 > 0$  direct photon processes are not sufficient to describe the data. Additional processes, like the contribution of resolved virtual photons, are needed to improve the description of the data.

#### 4 What did we learn?

We have seen that the concept of resolved virtual photons provides a good description of di-jet production in the region where  $E_T^2 > Q^2$ . However in general in DIS the situation is more complicated than in photo-production, because of the presence of two hard scales:  $E_T^2$  and  $Q^2$ . DIS processes may be separated into three different regions of phase space, depending whether

$Q^2$  or  $p_T^2$  is larger or both are of the same order. From the discussion of the forward jet cross section as function of  $E_T^2/Q^2$  it became clear, that the full phase space can be described using the concept of resolved virtual photons provided the scale of the hard subprocess is large enough:  $\mu^2 > E_T^2$ .

Thus, if we consider  $\mu^2 = E_T^2$  to be the proper hard scale, then deep inelastic scattering turns out to consist of three different pieces: the standard DIS region (pointlike photon) with  $Q^2$  being the largest scale, a typical resolved photon region where  $E_T^2$  is the largest scale, and then the typical BFKL region where  $Q^2 \sim E_T^2$ . Such a picture is quite unsatisfactory since it requires a proper treatment of the interplay of the contributions in the different regions of phase space as well as the problem of possible double counting. However all the difficulties in describing the data come from the approximations used in the evolution of the parton densities and the calculation of the hard scattering matrix elements: the leading  $\log Q^2$  - or collinear approximation. These problems can be overcome by using the  $k_T$  - factorization or semi-hard approach together with the CCFM<sup>15,16,17,18</sup> evolution equations for the parton densities, which reproduces the DGLAP and the BFKL equation in the appropriate limits. Since in the  $k_T$  - factorization approach the matrix elements are treated with off shell incoming partons, the anomalous component of the resolved photon is automatically included as soon as  $k_T^2$  becomes larger than  $Q^2$ . Recently it has been shown<sup>19,20,21</sup> that the cross section of forward jet production as a function of  $E_T^2/Q^2$  can be nicely reproduced within the CCFM framework. This gives confidence that we are on the way to obtain a unified picture of high energy deep inelastic lepton scattering.

## Acknowledgments

I am grateful to the organizers for this stimulating conference. I am also grateful to the Swedish Science Council (NFR) for financial support.

## References

1. H1 Collaboration, C. Adloff et al., *Phys. Lett.* **B** (2000) , DESY-00-035.
2. ZEUS Collaboration, J. Breitweg et al., *Eur. Phys. J.* **C 11** (1999) 35, DESY 99-057.
3. H1 Collaboration, C. Adloff et al., *Phys. Lett.* **B 415** (1997) 418, DESY-97-179.
4. J. Chyla, J. Cvach, in *Proc. of the Workshop on Future Physics at HERA*, edited by A. De Roeck, G. Ingelman, R. Klanner (Hamburg, 1996).
5. A. Mueller, *Nucl. Phys.* **B (Proc. Suppl)** **18C** (1990) 125.
6. A. Mueller, *J. Phys.* **G 17** (1991) 1443.
7. G. Kramer and B. Pötter, *Phys. Lett.* **B 453** (1999) 295.
8. ZEUS Collaboration, J. Breitweg et al., *Phys. Lett.* **B 474** (1999) 223.
9. G. Ingelman, A. Edin, J. Rathsman, *Comp. Phys. Comm.* **101** (1997) 108.
10. G. Marchesini et al., *Comp. Phys. Comm.* **76** (1992) 465, hep-ph/9912396.
11. H. Jung, in *Proc. of the Madrid low x workshop*, edited by F. Barreiro (Miraflores de la Sierra, Spain, 1997), hep-ph/9709425.
12. H1 Collaboration, C. Adloff et al., *Eur. Phys. J.* **C C13** (1998) 397, DESY-98-205.
13. ZEUS Collaboration, J. Breitweg et al., *Phys. Lett.* **B** (2000) , DESY 00-017.
14. B. Pötter, *Comp. Phys. Comm.* **119** (1999) 45 and hep-ph/9911221
15. M. Ciafaloni, *Nucl. Phys.* **B 296** (1988) 49.
16. S. Catani, F. Fiorani, G. Marchesini, *Phys. Lett.* **B 234** (1990) 339.
17. S. Catani, F. Fiorani, G. Marchesini, *Nucl. Phys.* **B 336** (1990) 18.
18. G. Marchesini, *Nucl. Phys.* **B 445** (1995) 49.

19. G. Marchesini, B. Webber, *Nucl. Phys.* **B 349** (1991) 617.
20. G. Marchesini, B. Webber, *Nucl. Phys.* **B 386** (1992) 215.
21. H. Jung, in *Proceedings of the Workshop on Monte Carlo generators for HERA physics*, edited by A. Doyle, G. Grindhammer, G. Ingelman, H. Jung (DESY, Hamburg, 1999), hep-ph/9908497.